J Chem Ecol (2011) 37:880–890
DOI 10.1007/s10886-011-9987-3

Effects of a Coumarin Derivative, 4-Methylumbelliferone, on Seed Germination and Seedling Establishment in *Arabidopsis*

Xiang Li · Margaret Y. Gruber · Dwayne D. Hegedus · Derek J. Lydiate · Ming-Jun Gao

Received: 17 March 2011 / Revised: 8 June 2011 / Accepted: 10 June 2011 / Published online: 29 June 2011

Abstract The root system is central for plant adaptation to soil heterogeneity and is organized primarily by root branching. To search for compounds that regulate root branching, a forward chemical genetics screen was employed, and 4-methylumbelliferone (4-MU), a coumarin derivative, was found to be a potent regulator of lateral root formation. Exogenous application of 4-MU to *Arabidopsis thaliana* seeds affected germination and led to reduced primary root growth, the formation of bulbous root hairs, and irregular detached root caps accompanied by reorganization of the actin cytoskeleton in root tips before seedling establishment. Abundant lateral roots formed after exposure to 125 μM 4-MU for 22 days. Molecular, biochemical, and phytochemical approaches were used to determine the effect of 4-MU on root growth and root branching. *Arabidopsis* seedlings grown in the presence of 4-MU accumulated this compound only in roots, where it was partially transformed by UDP-glycosyltransferases (UGTs) into 4-methylumbelliferyl-β-D-glucoside (4-MU-Glc). The presence of 4-MU-Glc in seedling roots was consistent with the upregulation of several genes that encode UGTs in the roots. This shows that UGTs play an integral role in the detoxification of 4-MU in plants. The increased expression of two auxin efflux facilitator genes (*PIN2* and *PIN3*) in response to 4-MU and the lack of response of the auxin receptor *TIR1* and the key auxin biosynthetic gene *YUCCA1* suggest that auxin redistribution, rather than auxin biosynthesis, may directly or indirectly mediate 4-MU-induced root branching.

Key Words Coumarin · 4-methylumbelliferone · Glycosyltransferases · Detoxification · Lateral root

Introduction

Plants are sessile and must endure environmental challenges, which include changes in water and nutrient availability and their heterogenous distribution in the soil. To acquire water and nutrients efficiently, plants dynamically modulate their root systems by regulating primary root growth, lateral root formation, and root hair number (de Dorlodot et al., 2007; Osmont et al., 2007; Nibau et al., 2008). Although progress has been made in dissecting the hormonal, genetic, and nutritional control of lateral root development (de Dorlodot et al., 2007; Osmont et al., 2007; Nibau et al., 2008; Peret et al., 2009), the mechanisms underlying the initiation and emergence of lateral roots are unclear. The formation of lateral roots is dependent on the coordinated action of many factors. In *Arabidopsis thaliana*, more than seventy genes have been shown to influence lateral root development (De Smet et al., 2006); however, the plant hormone auxin and its polar transport and redistribution have emerged as key factors (Fukaki et al., 2002; Nibau et al., 2008; Peret et al., 2009; Vanneste and Friml, 2009). Intercellular auxin movement is controlled by several plant-specific pin-formed (PIN) proteins that facilitate auxin efflux (Vanneste and Friml, 2009).

Electronic supplementary material The online version of this article (doi:10.1007/s10886-011-9987-3) contains supplementary material, which is available to authorized users.

X. Li
College of Plant Sciences, Jilin University, Changchun 130062, China

X. Li · M. Y. Gruber · D. D. Hegedus · D. J. Lydiate · M.-J. Gao (✉)
Agriculture and Agri-Food Canada, Saskatoon Research Centre, Saskatoon, Saskatchewan S7N 0X2, Canada
e-mail: Ming-Jun.Gao@agr.gc.ca

Coumarins (1, 2-benzopyrones) are secondary metabolites often found in roots of higher plants where they originate from the general phenylpropanoid pathway (Bourgaud et al., 2006). While their exact biological function in plants remains unclear, historically they are known to be involved in plant defense (Baumert et al., 2001; Carpinella et al., 2005; Brooker et al., 2007) along with flavonoids, phenolics, and alkaloids. Unlike most other secondary metabolites, coumarins appear to specifically inhibit seed germination and root growth (Svensson, 1971; Abenavoli et al., 2001, 2004, 2006, 2008; DeBolt et al., 2007), and this is consistent with previous observations that coumarins accumulate mainly in roots. They also influence membrane transport in the root tip (Lupini et al., 2010) and nitrogen uptake and metabolism (Abenavoli et al., 2001, 2003). Some natural coumarins also have received attention for their pharmacological properties, such as inhibition of HIV-1 and in treating thromboembolic diseases (Kostova et al., 2006).

Chemical genetics has been used extensively in plant biology for the identification of metabolites and their candidate genes involved in specific biochemical pathways (Blackwell and Zhao, 2003). As part of our efforts to characterize natural products that affect seed germination, root growth, and root architecture, we used forward chemical genetics to screen a small-molecule chemical library. Here, we focused on a coumarin derivative, 4-methylumbelliferone (4-MU), which inhibited germination and primary root growth, but promoted root branching after seedling establishment. We investigated the role of this compound on these parameters in more detail and demonstrated that 4-MU specifically accumulates in roots, where it is transformed into 4-methylumbelliferyl-β-D-glucoside (4-MU-Glc) by the action of UDP-glycosyltransferases (UGTs). We propose that UGTs play an integral role in the biochemical detoxification of 4-MU in *Arabidopsis* during seed germination and seedling development.

Methods and Materials

Plants, Chemicals and Forward Chemical Genetic Screens All chemical standards were purchased from Sigma-Aldrich (St. Louis, MO, USA). Solvents used were high-pressure liquid chromatography (HPLC) grade. *Arabidopsis thaliana* ecotype Columbia (Col-0) was obtained from the *Arabidopsis* Biological Resource Center (Columbus OH, USA). Seeds were cold-treated at 4°C for 2 d before germination. A collection of 128 natural compounds was screened by germinating and growing *Arabidopsis* on sterile Murashige and Skoog (MS) medium (Sigma) supplemented with 1.2% agarose and 0, 25, 50, or 125 μM compound. Germination and seedling growth were conducted in a growth cabinet with 16 hr of light (22°C), 8 hr dark (18°C) and 60% relative humidity. Plants were grown for different lengths of time in 4-MU MS media based on the objectives of the experiments. For observation of 4-MU effects on seed germination and primary root growth, plants were treated for 6 d. For auxin transport analysis and MUG assays in root systems, plants were harvested after treatment for 14 d when lateral root branching has been initiated and *DR5::GUS* was actively expressed (Supplementary Data Fig. 1). To measure the effect of 4-MU on seedling establishment and root architecture, plants were treated for up to 22 d when seedlings and root branching were well established. Fresh weight and root length were measured immediately after harvest. The *35S::ABD-GFP* (Motes et al., 2005) construct was provided by Dr. Elison B. Blancaflor, and the *DR5::GUS* transgenic line (Ulmasov et al., 1997) by Dr. Tom Guilfoyle (University of Missouri).

GUS Expression Analysis Quantitative analysis of GUS activity was conducted using 4-methylumbelliferyl β-D-glucuronide hydrate (MUG) fluorometric assays (Jefferson, 1987). Seedlings (200 mg) were ground with 1 ml of GUS extraction buffer containing 0.1 M Na_2HPO_4 (pH 7.5), 10 mM EDTA, 0.1% Triton X-100, and 10 mM β-mercaptoethanol at 4°C. After centrifugation, 100 μl of the extract were incubated with 2 mM MUG in extraction buffer in a final volume of 1 ml for 3 hr at 37°C. Three independent replicates were conducted.

Fluorescent Confocal Microscopy Laser scanning confocal and differential interference contrast microscopy was performed with a Carl Zeiss LSM150 microscope (Department of Veterinary Biomedical Sciences, University of Saskatchewan). GFP fluorescence was detected using excitation and emission wavelengths of 488 and 505 nm, respectively. The data shown are representative of three independent experiments. The images were analyzed using NIH Image J 1.37 software (http://rsb.info.nih.gov/ij/).

Identification and Purification of 4-MU-O-β-D-Glucopyranoside Arabidopsis roots were harvested and frozen at −80°C from plants grown 6 d either in the presence or absence of 4-MU. A 100 mg sample of frozen roots was ground in liquid nitrogen in a 20 ml Potter-Elvehjem, followed by grinding in 10 ml methanol/water (80:20; v/v) for 10 min. After filtration, the pellet was extracted again with methanol/water overnight at 4°C in the dark. The two extracts were combined and dried at 35°C under vacuum, and the dried extract was resuspended at 1 mg ml^{-1} with methanol/water (50:50; v/v). HPLC/UV analysis was conducted using a Hewlett Packard Agilent 1100 chromatograph, a G-7120 diode array detector, HP Chemstation ver. 08.01 software and a Zorbax C_{18} column

(150×4.6 mm, 5 μm, Mississauga, ON, Canada) with a 60 min linear gradient of 5–75% methanol v/v, a flow rate of 1.0 ml min^{-1}, and an injection volume of 2 μl. LC-MS profiles were obtained on an Agilent 1100 HPLC and an API QStar XL pulsar hybrid system (Applied Biosystems, Foster City, CA, USA) (Li et al., 2011).

Identical chromatography conditions were used for semi-preparative purification of 4-MU-*β*-D-glucoside (4-MU-Glc) from 5 g of 4-MU-treated frozen root tissue, except that the flow rate was 3.0 ml min^{-1} and a Zorbax C_{18} column (150 mm x 2.5 cm, Mississauga, ON, Canada) was used. The major peak was isolated, dried in a rotary evaporatory, and then the compound was dissolved in 510 μl of fresh methanol (Sigma). ^{1}H NMR, ^{1}H-^{1}H COSY, and HMBC spectra were measured on the isolated compound with a Bruker Advance 500 NMR spectrometer equipped with a Bruker 5 mm inverse tripe resonance TXI probe (Bruker Biospin, Rheinstetten, Germany) at the Saskatchewan Structural Science Centre, University of Saskatchewan. Chemical shifts (Table 1) (δ) were expressed in parts per million (ppm) and coupling constants (*J*) in Hertz (Hz).

To determine the configuration of the sugar moiety, the isolated compound was refluxed with 6 N HCl (5 ml) at 100°C for 2 h (Li et al., 2009b). The mixture was extracted with $CHCl_3$ to remove the aglycone, then the aqueous layer was neutralized with Na_2CO_3, filtered, and dried under vacuum. A portion of the aqueous residue was dissolved in H_2O for sugar analysis by thin layer chromatography (TLC) (Macherey-Nagel, SilG/UV254, 0.20 mm) with n-BuOH: HOAc:H_2O (6:1:2) as the solvent. TLC sample spots were detected by spraying aniline hydrogen phthalate reagent (100 ml n-butanol saturated by H_2O, 0.96 g aniline and 1.66 g phthalic acid) and heating. The absolute configuration of glucose was determined by chiral GC-FID analysis using an Agilent GC and a 0.25 mm×25 mm Hydrodexb-6-TBDM chiral capillary column (Macherey-Nagel, Germany). *β*-D-glucose (Sigma) was used as an authentic GC standard. A portion of the aqueous layer residue also was resuspended in 1 ml dichloromethane followed by the addition of 50 μl trifluoroacetic anhydride. The mixture was allowed to react at room temperature for 16 h and dried under a stream of nitrogen at room temperature. The sugar derivative was separated on the GC using the following temperature program: inlet temperature at 240°C; hydrogen carrier gas and a 1/20 split using nitrogen as the makeup gas; column temperatures starting at 120°C, ramping to 220°C at 50°C min^{-1} and maintenance for 12 min.

Microarray Total RNA was extracted from *Arabidopsis* seedlings grown on agar plates for 6 d with or without 4-MU supplementation using the RNeasy plant mini kit (Qiagen, Valencia, CA, USA). cDNA was prepared using Superscript II reverse transcriptase (Invitrogen, Carlsbad, CA, USA) according to the manufacturer's instructions. Three biological replicates were collected for each sample. An *Arabidopsis* 26 K cDNA array (Qiagen, Valencia, CA, USA) was hybridized with Cy5- and Cy3-labelled probe pairs from the 4-MU treated and untreated samples. Probe labeling, hybridization, and washing were conducted using a CyScribe Post-Labeling kit according to the manufacture's instruction (Amersham Biosciences, Pittsburgh, PA, USA). Hybridized slides were scanned on a GenePix 4000B scanner (Axon Instruments Inc., Union City, CA, USA). The intensity (I) of each spot at λ_{546nm} and λ_{647nm} was transformed into a I_{546}:I_{647}ratio with Array-Pro Analyzer 4.0 (Media Cybernetics Inc., Bethesda, MD, USA). Microarray data initially were imported into BASE 1.2.16. The data then were filtered, normalized, and analyzed with Gene-Spring 6.1 (Silicon Genetics, Redwood City, CA, USA) as previously described (Zhao et al., 2009), and imported into MapMan for category analysis.

Real Time RT-PCR mRNA from the microarray experiment was converted to cDNA with SuperScript III First-Strand Synthesis SuperMix (Invitrogen, Carlsbad, CA, USA) according to the manufacturer's instructions. Quantitative real time PCR analysis (qRT-PCR) was carried out using a Platinum SYBR Green qPCR SuperMix-UDG kit (Invitrogen, Carlsbad, CA, USA) on an ABI PRISM StepOnePlus Real-Time PCR System (Applied Biosystems) as previously described (Gao et al., 2009; Li et al., 2011). The *Arabidopsis*

Table 1 ^{1}H-NMR data of 4-MU and 4-MU-Glc (500 MHZ) [a, b]

	4-MU	4-MU-*O*-*β*-*D*-Glc		4-MU	4-MU-*O*-*β*-*D*-Glc
2	–	–	10	–	–
3	6.10, *s*	6.10, *s*	-CH_3	2.43, *s*	2.36, *s*
4	–	–	1′	–	4.95, *d*, 7.6
5	7.59, *d*, 8.5	7.62, *d*, 8.5	2′	–	3.32–3.45, *m*
6	6.83, *dd*, 8.5, 1.7	7.04, *dd*, 8.5, 1.7	3′	–	3.32–3.45, *m*
7	–	–	4′	–	3.32–3.45, *m*
8	6.70, *d*, 1.7	6.97, *d*, 1.7	5′	–	3.64, *dd*, 11.8, 5.6
9	–	–	6′	–	3.82, *d*, 11.8

[a] Spectra were measured in MeOD, and chemical shifts are expressed in ppm

[b] Multiplicity and *J* values in Hz are given in parentheses

Ef-1α gene was chosen as an endogenous reference gene. Primer sequences for qRT-PCR were designed using Oligo Perfect Primer Design software provided by Invitrogen (http://tools.invitrogen.com/) (Table 2). For each pair of primers, gel electrophoresis and melting curve analyses were performed to ensure that only a single PCR amplicon of the expected length and melting temperature was generated. Each sample was assayed in triplicate, and data were analyzed using Step-One v2.0 (Applied Biosystems). The level of each mRNA was calculated using the mean threshold cycle (Ct) value and normalized to that of the reference gene *Ef-1α*. All results are shown as means of at least three biological replicates with corresponding standard deviations (SD).

Glucosyltransferase Activity Assay To generate constructs for GST-UGT expression, the full length open reading frames (ORFs) of *UGT73B4* and *UGT75B2* were amplified by PCR using primers 73B4-PET-F and 73B4-PET-R for *UGT73B4* and primers 75B2-PET-F and 75B2-PET-R for *UGT75B2* (Table 2), and cloned into the pET102/D/TOPO vector using the directional TOPO cloning system (Invitrogen, Carlsbad, CA, USA). All constructs were confirmed by DNA sequencing. The recombinant plasmids were transformed into *Escherichia coli* BL21 Star (DE3) cells (Invitrogen, Carlsbad, CA, USA), and the protein was purified as a GST fusion according to the manufacturer's instructions (Qiagen, Valencia, CA, USA). Each glucosyltransferase activity assay mix (2 ml) contained 100 μg of recombinant protein, 50 mM Tris-HCl, pH 7.0, 10 mM β-mercaptoethanol, 10 mM UDP-glucose, and 1 mM 4-MU as substrate. The reaction mix was incubated at 28°C for 1 h, stopped with the addition of 200 μM trichloroacetic acid, and subjected to reverse-phase HPLC analysis as described above. Absorbance at λ_{320} was used to monitor chromatogram profiles, and the identity of peaks (compounds) was confirmed by comparing retention times and photo-diode array profiles with authentic standards.

Statistical Analysis All experiments were conducted in triplicate and mean data (±SD) analyzed with ANOVA for significance (LSD at $P<0.05$) using SAS 9.0 (SAS Institute, Inc. Cary, NC, USA), unless otherwise indicated. For microarray analysis, log ratios of intensity after

Table 2 Primers used in this study

	Gene	AGI code	Sequences
GAUT2-F	*GAUT2*	AT2G46480	CCTGCCTTTACCGATGAGAA
GAUT2-R			AAGGTGGAAAACATGCCTTG
UGT73B4-F	*UGT73B4*	AT2G15490	GGAGAAGATCGGTGTTCCAA
UGT73B4-R			CAGGGAGACCAGGGATTACA
UGT73C1-F	*UGT73C1*	AT2G36750	CGCACATAATGCACCAAAAC
UGT73C1-R			CCGTCAAGGAAGTCTTTCCA
UGT75B2-F	*UGT75B2*	AT1G05530	GACACCGAGCCATAGGTTGT
UGT75B2-R			CCCTCACACCTGTCTTCCAT
PIN2-F	*PIN2*	AT5G57090	CCATGATAACGCCGCGAGCTTC
PIN2-R			TGACGAGGGCTTGGAGCTTTGC
PIN3-F	*PIN3*	AT1G70940	CCATCTTCGCCGTCCCTCTCCT
PIN3-R			CGAGGCTACCGGAGCGAGTGAA
IAA14-F	*IAA14*	AT4G14550	AAAGTCCGGCCAAGTCGGGTGT
IAA14-R			CCTCTGCTTCGCCGCTCTTCTG
GH3-F	*GH3*	AT2G14960	CGTTGCTGCCTTGGGATGGAAG
GH3-R			GGGCTAAAATGCGCCGACACAA
YUCCA1-F	*YUCCA1*	AT4G32540	ATCGGAGCTGGCCCTTCTGGTC
YUCCA1-R	*TIR1*	AT3G62980	CCAGGAGGGGTAACCGGCAAAA
TIR1-F			ATCGGGAACTGCTACGCCGTGA
TIR1-R			TCCAAGCAATCGTCGGTGACCA
EF-1α-F	*EF-1α*	AT1G07920	GCAAGGGCCTCAGCTCTG
EF-1α-R			ACAAGCCGTCTGGGTATATGTTAGC
73B4-PET-F	*73B4-PET*	AT2G15490	CGCTCGAGATGAACAGAGAGCAAATTCATA
73B4-PET-R			CGGAATTCCTACTTTCTACCATTCAGCTCTTC
75B2-PET-F	*75B2-PET*	AT1G05530	CGCTCGAGATGGCGCAACCGCATTTT
75B2-PET-R			CGGAATTCTCAAAACAGACTCTTCACAA

background correction were scaled to have similar distribution across and consistency among arrays. The ANOVA model "log $(y_{ijkgr})=\mu+A_i+D_j+T_k+G_g+AG_{ig}+DG_{jg}+TG_{kg}+\varepsilon_{ijkr}$" was employed to detect differentially expressed genes using the normalized data, where log (y_{ijkgr}) represents the background-corrected and normalized natural logarithm of the intensity of the r^{th} replicate of gene g on array i, with dye j, and treatment/condition k; μ represents the average natural logarithm of gene intensity over all the genes, arrays and dyes; A, D, T, and G represent the array, dye, treatment and main gene effect, respectively; and ε_{ijkr} represents normal distribution with mean zero (Li et al., 2009a).

Results

Identification of 4-MU as a Root Growth Effector A set of 128 natural compounds was screened for their impact on *Arabidopsis* seed germination, primary root growth, root architecture, and seedling establishment. Out of this screening, seven coumarins and five phenolic acids delayed *Arabidopsis* seed germination and inhibited root growth. One coumarin and two ginsenosides inhibited root growth alone, and one phenolic acid and one flavonoid inhibited seed germination alone (Supplementary Table 1). Of all compounds tested, 4-MU affected all three parameters, including root architecture. Since 4-MU was the only compound to affect root architecture, it became the focus of the remainder of this study

Seed germination was inhibited by a range of 4-MU treatments. Germination rates were 90% and 75% with 125 μM and 250 μM 4-MU, respectively. Seeds were unable to germinate when the concentration of 4-MU was increased to 500 μM (data not shown). Primary root growth was inhibited in 6-d-old seedlings grown on medium supplemented with 125 μM or 250 μM 4-MU (Fig. 1a,b,c). Primary root length was reduced by 25% and 75%, respectively, compared to untreated control seedlings over a 22 d time period (Fig. 2a), but growth of cotyledons, hypocotyls and rosette leaves was not affected at these concentrations (Figs. 1a,b, c and 2b). Accompanying the negative effect on primary root growth, the development of root hairs on primary roots also was affected by 4-MU. Approximately 20% of root hairs on primary roots were bulbous at 125 μM 4-MU (Fig. 1h), while very few root hairs were fully emerged at 250 μM 4-MU (Fig. 1i). After exposure to 125 μM 4-MU, lateral roots began to form as buds by day 14, and abundant lateral roots had formed by 22 days, even though primary root growth was hindered (Fig. 2c). Since accumulation of coumarins can be detected in plant tissues under UV light (Chong et al., 2002; Kai et al., 2008), the 6-d-old *Arabidopsis* seedlings grown on media supplemented with 4-MU were compared with untreated roots under UV light. Consistent with the

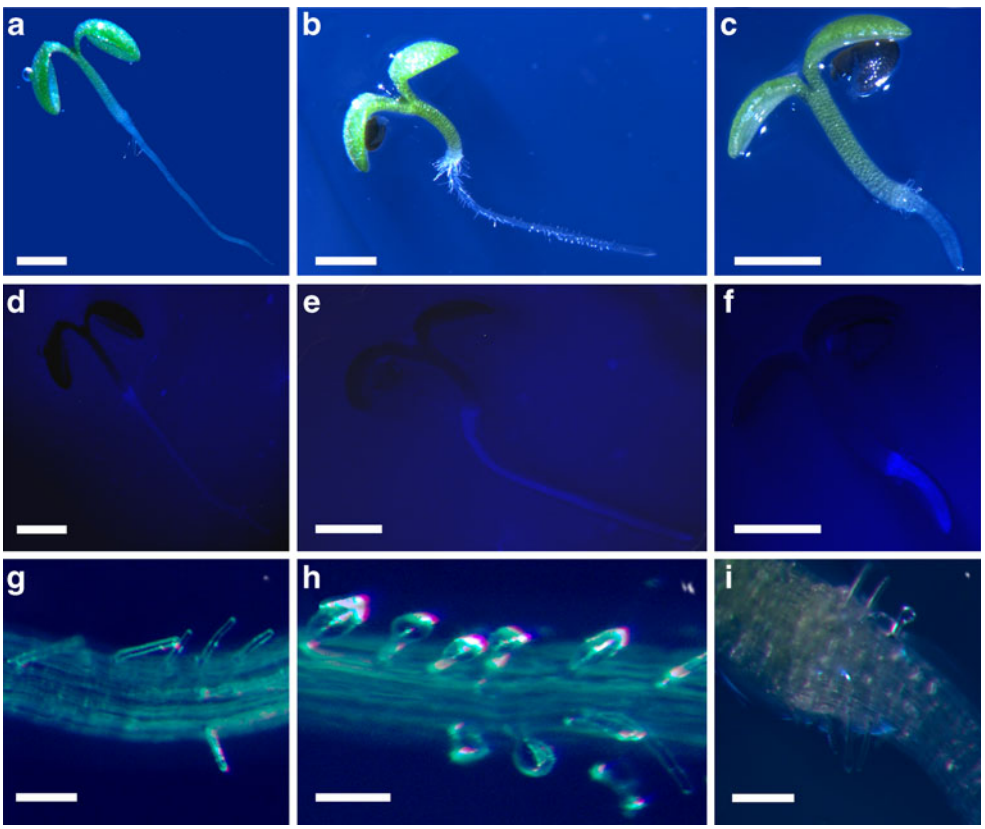

Fig. 1 The effect of exogenous 4-MU on growth of primary roots. *Arabidopsis* seedlings were grown vertically on media supplemented with different concentrations of 4-MU for 6 d. **a** An untreated seedling. **b** A seedling treated with 125 μM 4-MU. **c** A seedling treated with 250 μM 4-MU. (**d**, **e** and **f**) UV (325 nm) channel of (**a**), (**b**) and (**c**) showing the accumulation of fluorescent 4-MU in primary roots. (**g**, **h** and **i**) Root hairs of (**a**), (**b**) and (**c**) showing bulbous root hairs on the primary root after treatment with 125 μM 4-MU, and inhibition of root hair formation after treatment with 250 μM 4-MU. Scale bars in **a**–**f**, 1 cm; in **g**–**i**, 2 mm

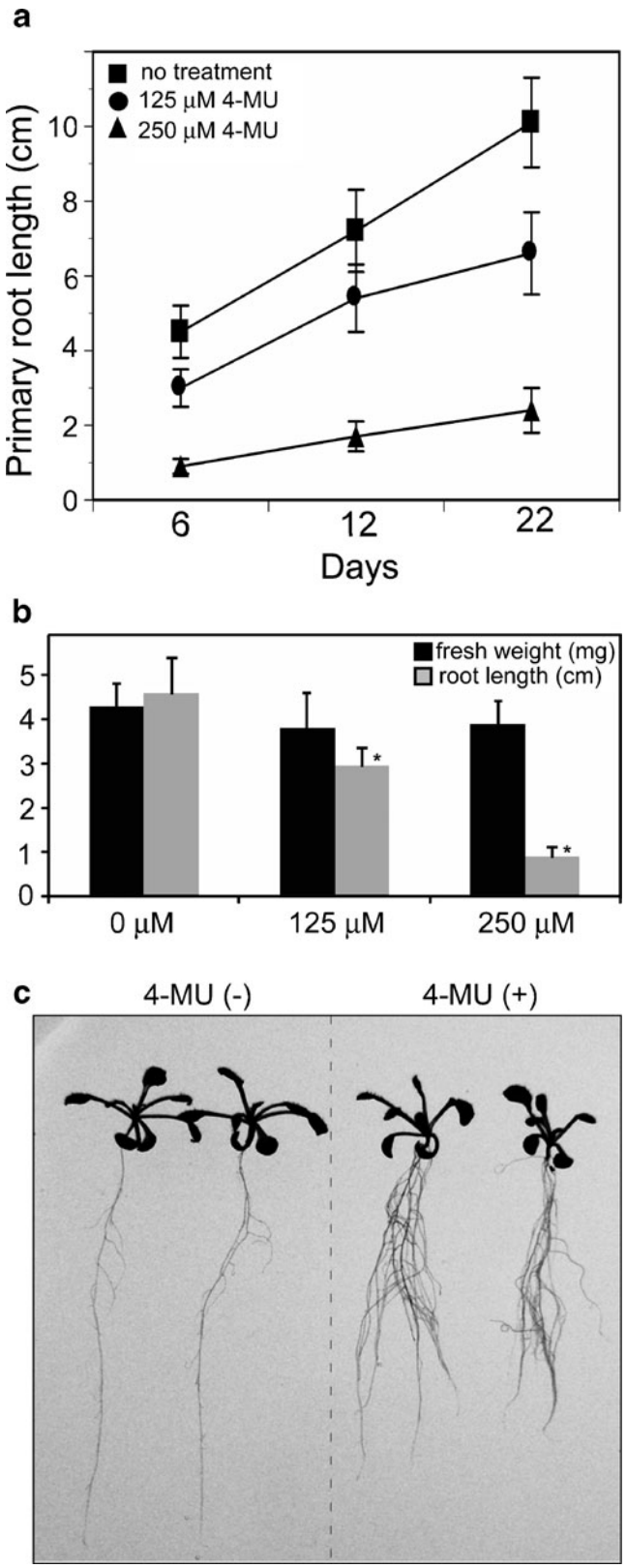

Fig. 2 The effect of 4-MU on *Arabidopsis* growth. **a** Time course of the effect of 4-MU on primary root elongation over 22 d. Values represent the means±SD of three replicates. **b** Fresh weight of aerial parts of plants (mg FW per 10 seedlings without roots) and root length (cm) of 6-d-old plants in the presence or absence of 4-MU. Data represent the mean±SD from 6 independent experiments. Asterisks indicate significant difference between treated and untreated plants based on a student test ($P<0.05$). **c** Root system architecture and aerial vegetation of 22-d-old plants showing root branching in the presence (right) of 125 µM 4-MU, very little branching without 4-MU (left), and normal rosette growth under both conditions

inhibition of *Arabidopsis* root growth by 4-MU, blue fluorescence increased in roots of seedlings treated with this compound (shown for 250 µM 4-MU in Fig. 1e and f).

Accumulation and Glucosylation of 4-MU in Arabidopsis Roots To confirm the presence of 4-MU in *Arabidopsis* roots, we analyzed the phytochemical composition of roots of 6-d-old seedlings by HPLC-UV/MS. In MeOH extracts from roots exposed to 125 µM 4-MU, 4-MU and a large additional peak were detected at *Rt* 36.5 min and *Rt* 23.0 min, respectively. Neither of these peaks was detected in the roots of untreated seedlings (Fig. 3a). Comparison of the ^{1}H NMR spectrum of the new reaction product with that of 4-MU (Supplementary Data Figs. 2 and 3) showed no significant chemical shifts in the aromatic proton signals, but an additional set of sugar moiety signals appeared at δ 4.95 (1H, *d*, J=7.6 Hz), 3.82 (1H, *d*, J=11.8 Hz), 3.62 (1H, *dd*, J=5.6, 11.8 Hz), and 3.32-3.45 (3H, m) (Table 1). Combinational ^{1}H-^{1}H COSY and HMBC NMR spectra (Supplementary Data Figs. 4 and 5) were used to elucidate the structure. The sugar moiety was identified as glucose on the basis of an acid hydrolysis reaction, which gave a reaction product with the same R_f on a TLC plate as an authentic glucose standard compound (data not shown). The coupling constant $J_{H1', H2'}$ (7.6 Hz) of the new enzyme reaction product, followed by chiral GC analysis, indicated an absolute configuration of β-D-glucose. The new reaction product was defined as $C_{16}H_{18}O_8$ [4-MU-β-D-glucopyranoside (4-MU-Glc)] based on its HRESIMS ($[M+Na]^+$, *m/z* 361.0906, calc. 361.0899) (Fig. 3b). This indicates that 4-MU is partially transformed into 4-MU-Glc by glucosylation after uptake in *Arabidopsis* roots.

To gain additional insight into how *Arabidopsis* plants react to 4-MU by glucosylation after seed germination, we conducted a microarray analysis of 6-d-old seedlings grown on medium containing 125 µm 4-MU (Supplementary Data Tables 2 and 3). A total of 316 genes showed statistically significant up-regulation, while 243 showed statistically significant down-regulation. Genes determined to be up-regulated or down-regulated ≥ 2-fold in the treated relative to the untreated sample were catalogued and placed into twelve categories based on gene function according to *Arabidopsis* Gene Ontology (Supplementary Data Fig. 6). Although differences between treated and untreated samples were noted for individual genes, the number of up-regulated and down-regulated genes were similar in the categories of response to stress (51 vs. 48), response to

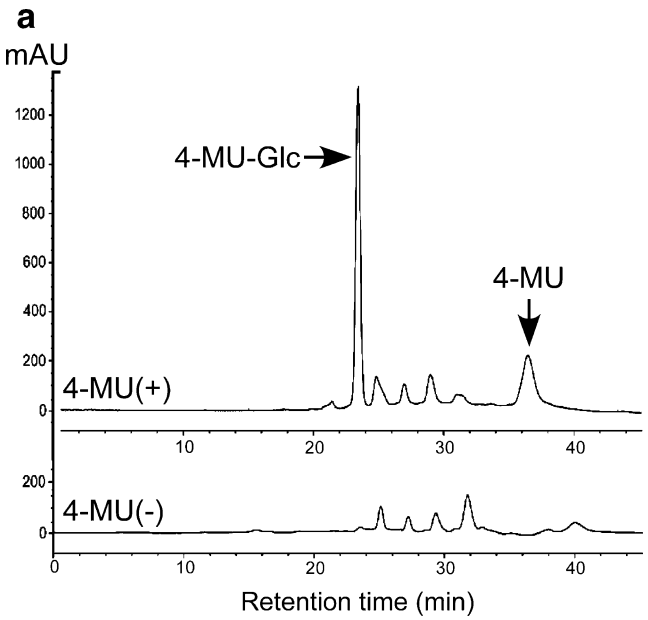

Fig. 3 Glucosylation of 4-MU in *Arabidopsis* roots. **a** HPLC-UV profiles (λ_{325}) of 80% methanol extracts from roots of 6-d-old seedlings treated with (upper panel) or without (bottom panel) 125 μM 4-MU. A new product was identified as 4-MU-*β*-D-glucoside (4-MU-Glc) in the 4-MU treated root extracts. **b** Schematic of the UGT-catalyzed biotransformation of 4-MU to 4-MU-Glc in *Arabidopsis* roots

abiotic and biotic stresses (49 vs. 44), and transportation (32 vs. 25), respectively. It was notable that most of the genes with altered expression did not have known functions (99 vs. 145, respectively). Four genes encoding uridine diphosphate (UDP) glycosyltransferases (UGTs) were up-regulated more than two-fold in the 4-MU treated seedlings, these included *UGT73B4*, *UGT73C1*, *UGT75B2*, and *GAUT2* (At2g46480). Consistent with the microarray data, qRT-PCR analysis revealed significant up-regulation of these four *UGT* genes in roots of 6-d-old seedlings exposed to 125 μm 4-MU (Fig. 4). Since UGT73B4, UGT73C1, and UGT75B2 are active on hydroxycoumarins, scopoletin, and esculetin (Lim et al., 2003), we tested whether 4-MU could be glucosylated by these UGTs using purified recombinant UGT73B4 and UGT75B2 enzymes. Reverse-phase HPLC

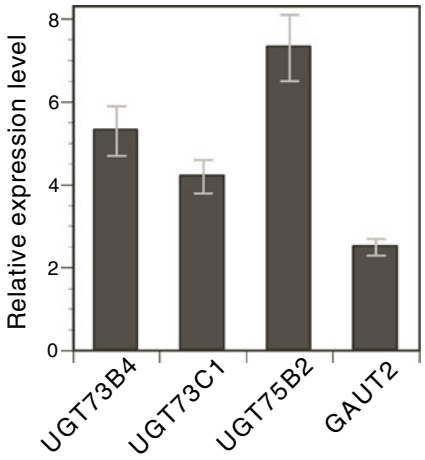

Fig. 4 Induction of glycosyltransferase genes by 4-MU in *Arabidopsis* roots. Quantitative RT-PCR analysis was used to analyze expression of genes encoding glycosyltransferases in the roots of 6-day-old seedlings treated with 125 μM 4-MU relative to levels from untreated seedlings. *Ef-1α* was used as a reference gene

and the identification of compounds in the post-reaction mixture showed a product with a retention time (22.1 min) and a photo-diode array profile identical to the authentic standard 4-MU-Glc in the reaction with UGT73B4, indicating that 4-MU is a substrate of this UGT (Fig. 5). UGT75B2 enzyme activity was not detected with 4-MU (data not shown).

Involvement of Auxin Efflux in 4-MU-Induced Lateral Root Formation Auxin plays a key role in controlling lateral root

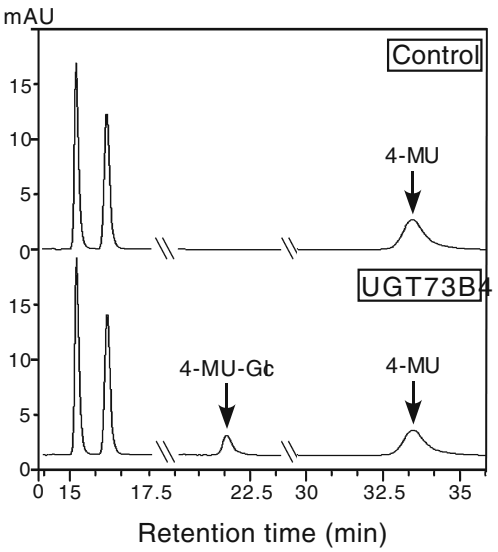

Fig. 5 HPLC-UV profiles of the reaction products of UGT73B4 recombinant protein incubated with 4-MU. Reaction products of GST protein (Control) or GST-UGT73B4 fusion (UGT73B4) were subjected to HPLC analysis and the products were detected at λ_{320}, (RT, 22.1 min) and confirmed by NMR, showing that UGT73B4 catalyzes the conversion of 4-MU to a 4-MU-Glc

formation (Fukaki and Tasaka, 2009). To test whether lateral root formation induced by 4-MU treatment was accompanied by an alteration in auxin signaling, we performed qRT-PCR analysis on genes involved in either auxin signal transduction, flux, or biosynthesis using total RNA extracted from 4-MU-treated roots of 14-d-old seedlings when lateral root branching has been initiated and *DR5::GUS* was actively expressed (Supplementary Data Fig. 1). For auxin flux facilitator genes, we chose *PIN2* and *PIN3* in preference to the other five *PIN* genes, which have additional or other functions. For example, *PIN1* is involved in vascular development, phyllotaxis, vein formation, embryogenesis, and lateral organ development (Petrásek and Friml 2009). *PIN2* and *PIN3* were up-regulated by 4-MU, whereas the expression of an auxin receptor *TIR1*, a rate-limiting for the auxin biosynthetic gene *YUCCA1* (Zhao et al., 2001), and an auxin-responsive GH3 family member At2g14960 (Mishra et al., 2009) was unchanged relative to untreated seedlings (Fig. 6a). Additionally, the transcript level of *IAA14/SLR1*, one of the most important auxin responsive AUX/IAA genes involved in lateral root initiation (Fukaki et al., 2002; Fukaki and Tasaka, 2009), was elevated by 4-MU. This analysis suggested that 4-MU affected auxin redistribution rather than biosynthesis. To eliminate the possibility that 4-MU treatment affects endogenous auxin biosynthesis, β-glucuronidase (GUS) activity under the control of the synthetic auxin-responsive promoter *DR5* (DR5::GUS) was determined in roots of 14-d-old seedlings grown on medium supplemented with 125 μM 4-MU. MUG activity (as measured by a fluorometric assay) in *DR5::GUS*—transformed *Arabidopsis* lines grown in the presence of 4-MU showed no difference compared to lines without 4-MU treatment (Fig. 6b), indicating that 4-MU had no effect on the regulation of auxin biosynthetic genes.

Alteration of Actin Filament Organization by 4-MU Treatment The actin cytoskeleton is important for root growth and is also thought to play a role in the polarization of auxin fluxes (Dhonukshe et al., 2008; Nick et al., 2009). We, therefore, examined the organization of the actin cytoskeleton system in roots in response to 4-MU. *Arabidopsis* plants were transformed with the actin-binding domain (ABD)-GFP protein fusion construct, which specifically binds filamentous (F)-actin (Motes et al., 2005) and allows visualization of the F-actin cytoskeleton. ABD-GFP florescence strongly accumulated in the root caps of untreated 6-d-old seedlings (Fig. 7b), whereas GFP fluorescence was observed in the meristematic tissues of seedlings treated with 125 μM 4-MU (Fig. 7e). Alteration of the root F-actin organization in plants treated with 125 μM 4-MU was accompanied by an abnormal root tip phenotype in which root caps appeared to be physically detached with irregularly shaped cells (Fig. 7d,f).

Discussion

We have characterized the response of the *Arabidopsis* root system to treatment with 4-MU. In the presence of this compound, seed germination was inhibited, primary root growth and root hairs were reduced, and lateral root emergence was stimulated, while cotyledons and seedling rosette leaves were unaffected (at least up to 22 days of evaluation). At high concentrations (500 μM), germination

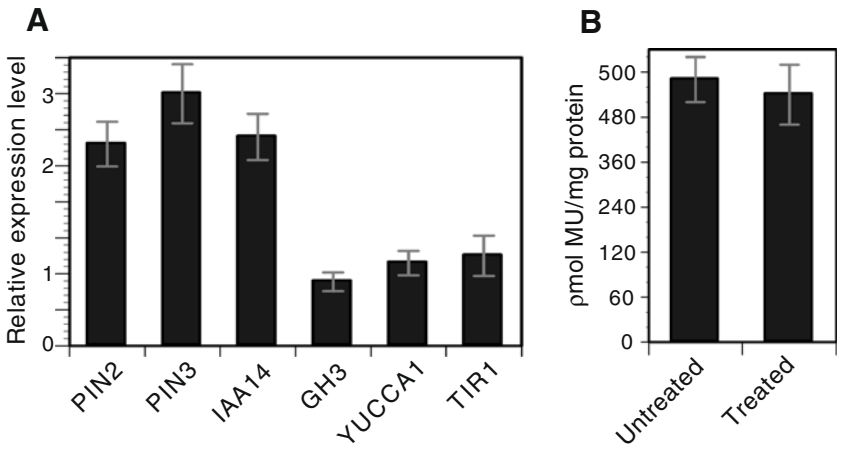

Fig. 6 (A) Transcript abundance of auxin biosynthesis, efflux, signalling, and responsive genes after 4-MU treatment. Expression was tested for the auxin efflux facilitators *PIN2* and *PIN3*, the auxin-responsive genes *IAA14* and *GH3* (At2g14960), the major auxin biosynthetic gene *YUCCA1* and the auxin receptor *TIR1*. Real time PCR was used to examine transcript levels of the six genes are relative to that in untreated *Arabidopsis* seedlings. *Ef-1α* was used as a reference gene. (B) Auxin biosynthesis as detected by GUS activity levels in *DR5::GUS* transgenic seedlings untreated or treated 125 μM 4-MU. Values are the means ± SD of triplicate samples

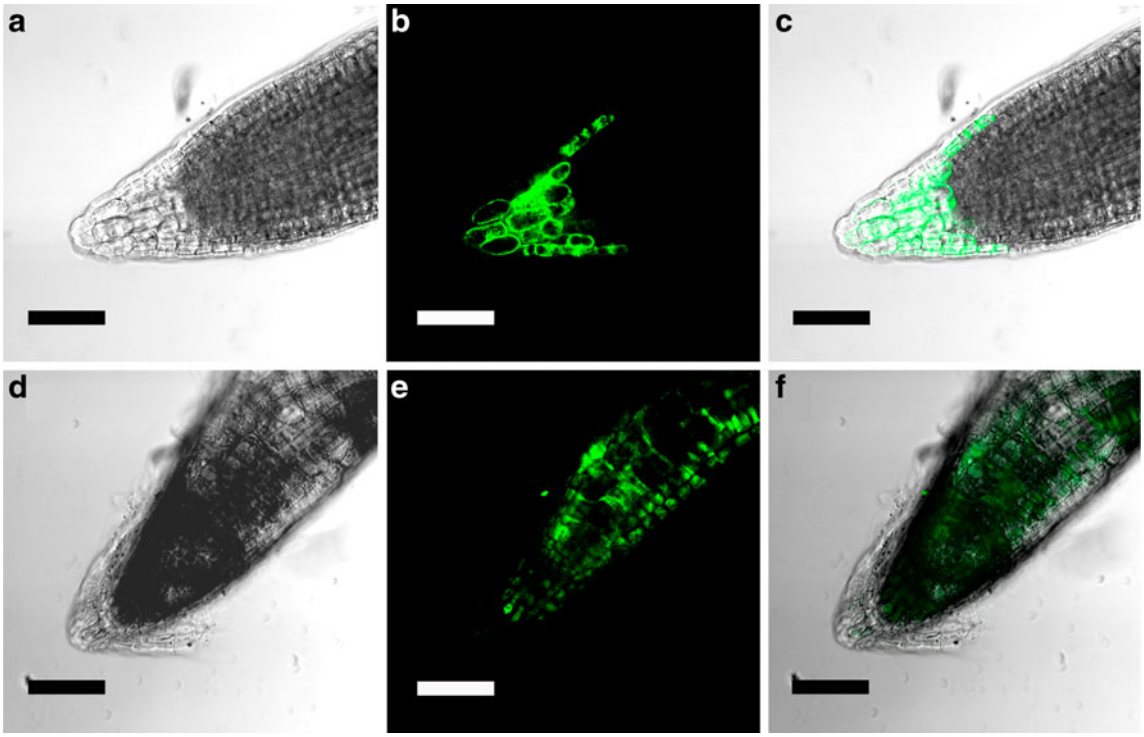

Fig. 7 Alteration of actin cytoskeleton organization in *Arabidopsis* root tips in response to 4-MU. Primary root tips of 6-d-old *35S::ABD-GFP* transformed seedlings were examined by fluorescence microscopy. (**a**, **b** and **c**) A root tip in the absence of 4-MU. (**d**, **e** and **f**) A root tip treated with 125 μM 4-MU. Brightfield (**a** and **d**), GFP channel (**b** and **e**), and merged (**c** and **f**) images are shown. Scale bar, 100 μm

was completely inhibited. Transcripts of three UGTs (UGT73B4, UGT73C1, UGT75B2) also were up-regulated after treatment with 4-MU, and a recombinant UGT73B4 enzyme could catalyze the glucosylation of 4-MU *in vitro* into the same end product (4-MU-Glc) that was accumulated with 4-MU *in vivo* in roots of the treated plants.

Plants have evolved complex pathways for responding to chemicals and toxins, such as glutathione sulphotransferase (GST)-catalyzed conjugation of glutathione and UGT-catalyzed glucosylation of diverse acceptors (Edwards et al., 2000; Gandia-Herrero et al., 2008). Glucosylation alters the properties of acceptor chemicals, such as their bioactivity, stability, hydrophilicity, and subcellular localization (Bowles et al., 2005). UGTs are involved in the synthesis and modification of glucoconjugates via transfer of sugars to a wide range of acceptor molecules that include plant secondary metabolites, phytotoxins, and xenobiotics (Bowles et al., 2005). UGT73B4 and several other UGTs have been shown to glucosylate coumarins, scopoletin, and esculetin, the flavonoid quercetin and 2,4,6-trinitrotoluene (TNT) (Lim et al., 2003; Gandia-Herrero et al., 2008). Hence, UGT-catalyzed glucosylation of 4-MU may represent a mechanism to inactivate this compound in *Arabidopsis* roots.

Auxin and its polar transport and redistribution are key factors controlling lateral root initiation, formation, and development (Nibau et al., 2008; Fukaki and Tasaka, 2009; Peret et al., 2009; Vanneste and Friml, 2009). Lateral root emergence was correlated with changes in auxin responsive gene expression in *Arabidopsis* challenged with 4-MU. Genes that encode the auxin efflux facilitators PIN2 and PIN3 were strongly up-regulated by 4-MU, and expression of the auxin receptor TIR1 or the key auxin biosynthetic enzyme YUCCA1 was unchanged in the presence of 4-MU. The F-actin fibrils in the primary root also were disrupted, and the root cap was detached under 4-MU exposure. These observations suggest that 4-MU induces lateral root emergence and root branching through auxin redistribution rather than auxin biosynthesis and does so in concert with (and as a consequence of) the inhibition of primary root growth.

Small compounds with impacts on cellular activity are useful, potent chemical tools for defining protein function (Walsh and Chang, 2006) and have provided insight into regulatory mechanisms, e.g., toyocamycin inhibition of auxin signaling (Hayashi et al., 2009). Our identification and characterization of 4-MU as a positive regulator of *Arabidopsis* root branching as a consequence of primary root inhibition is a starting point for continued chemical

genetics investigations aimed at identifying the cellular target of 4-MU. At this point, we also anticipate that 4-MU will prove to be a useful chemical tool for studying root biology and development in crop plants, particularly the *Brassicas* which are genetically close to *Arabidopsis*.

Acknowledgements X. Li was a recipient of a Visiting Fellowship to a Government Laboratory of Canada. The authors are grateful for technical assistance from Dr. Branimir Gjetvaj. We also thank Dr. Elison B. Blancaflor for providing the *35S::ABD2-GFP* construct and Drs. Elizabeth Schultz and Tom Guilfoyle for providing *Arabidopsis thaliana DR5::GUS* transgenic lines. This work was partially supported by the Program for New Century Excellent Talents in University (XL, NCET-09-0423), Ministry of Education of the People's Republic of China.

References

ABENAVOLI, M. R., DE SANTIS, C., SIDARI, M., SORGONA, A., BADIANI, M., and CACCO, G. 2001. Influence of coumarin on the net nitrate uptake in durum wheat. *New Phytol.* 150:619–627.

ABENAVOLI, M. R., SORGONÀ, A., SIDARI, M., BADIANI, M., and FUGGI, A. 2003. Coumarin inhibits the growth of carrot (*Daucus carota* L. cv. Saint Valery) cells in suspension culture. *J. Plant Physiol.* 160:227–237.

ABENAVOLI, M. R., SORGONÀ, A., ALBANO, S., and CACCO, G. 2004. Coumarin differentially affects the morphology of different root types of maize seedlings. *J. Chem. Ecol.* 30:1871–1883.

ABENAVOLI, M. R., CACCO, G., SORGONÀ, A., MARABOTTINI, R., PAOLACCI, A. R., CIAFFI, M., and BADIANI, M. 2006. The inhibitory effects of coumarin on the germination of durum wheat (*Triticum turgidum* ssp. *durum,* cv. Simeto) seeds. *J. Chem. Ecol.* 32:489–506.

ABENAVOLI, M. R., NICOLÒ, A., LUPINI, A., OLIVA, S., and SORGONÀ, A. 2008. Effects of different allelochemicals on root morphology of *Arabidopsis thaliana. Allelopathy J.* 22:245–252.

BAUMERT, A., MOCK, H. P., SCHMIDT, J., HERBERS, K., SONNEWALD, U., and STRACK, D. 2001. Patterns of phenylpropanoids in non-inoculated and potato virus Y-inoculation leaves of transgenic tobacco plants expressing yeast-derived invertase. *Phytochemistry* 56:535–541.

BLACKWELL, H. E., and ZHAO, Y. 2003. Chemical genetic approaches to plant biology. *Plant Physiol*. 133:448–455.

BOURGAUD, F., HEHN, A., LARBAT, R., DOERPER, S., GONTIER, E., KELLNER, S., and MATERN, U. 2006. Biosynthesis of coumarins in plants: a major pathway still to be unrevelled for cytochrome P450 enzymes. *Phytochem. Rev.* 5:293–308.

BOWLES, D., ISAYENKOVA, J., LIM, E. K., and POPPENBERGER, B. 2005. Glycosyltransferases: managers of small molecules. *Curr. Opin. Plant. Biol*. 8:254–263.

BROOKER, N. L., KUZIMICHEV, Y., LAAS, J., and PAVLIS, R. 2007. Evaluation of coumarin derivatives as anti-fungal agents against soil-borne fungal pathogens. *Commun. Agric. Appl. Biol. Sci.* 72:785–793.

CARPINELLA, M. C., FERRAYOLI, C. G., and PALACIOS, S. M. 2005. Antifungal synergistic effect of scopoletin, a hydroxycoumarin isolated from *Melia azedarach* L. fruits. *J. Agric. Food Chem.* 53: 2922–2927.

CHONG, J., BALTZ, R., SCHMITT, C., BEFFA, R., FRITIG, B., and SAINDRENAN, P. 2002. Down-regulation of a pathogen-responsive tobacco UDP-Glc: Phenylpropanoid glucosyltransferase reduces scopoletin glucoside accumulation, enhances oxidative stress, and weakens virus resistance. *Plant Cell* 14:1093–1107.

DE DORLODOT, S., FORSTER, B., PAGES, L., PRICE, A., TUBEROSA, R., and DRAYE, X. 2007. Root system architecture: opportunities and constraints for genetic improvement of crops. *Trends Plant Sci*. 12:474–481.

DEBOLT, S., GUTIERREZ, R., EHRHARDT, D. W., MELO, C. V., ROSS, L., CUTLER, S. R., SOMERVILLE, C., and BONETTA, D. 2007. Morlin, an inhibitor of cortical microtubule dynamics and cellulose synthase movement. *Proc. Natl. Acad. Sci. USA* 104:5854–5859.

DE SMET, I., VANNESTE, S., INZÉ, D., and BEECKMAN, T. 2006. LRI or the birth of a new meristem. *Plant Mol. Biol.* 60:871–887.

DHONUKSHE, P., GRIGORIEV, I., FISCHER, R., TOMINAGA, M., ROBINSON, D. G., HASEK, J., PACIOREK, T., PETRASEK, J., SEIFERTOVA, D., TEJOS, R., et al. 2008. Auxin transport inhibitors impair vesicle motility and actin cytoskeleton dynamics in diverse eukaryotes. *Proc. Natl. Acad. Sci. USA* 105: 4489–4494.

EDWARDS, R., DIXON, D. P., and WALBOT, V. 2000. Plant glutathione S-transferases: enzymes with multiple functions in sickness and in health. *Trends Plant Sci*. 5:193–198.

FUKAKI, H., and TASAKA, M. 2009. Hormone interactions during lateral root formation. *Plant Mol. Biol. Rep*. 69:437–449.

FUKAKI, H., TAMEDA, S., MASUDA, H., and TASAKA, M. 2002. Lateral root formation is blocked by a gain-of-function mutation in the SOLITARY-ROOT/IAA14 gene of *Arabidopsis*. *Plant J*. 29:153–168.

GANDIA-HERRERO, F., LORENZ, A., LARSON, T., GRAHAM, I. A., BOWLES, D. J., RYLOTT, E. L., and BRUCE, N. C. 2008. Detoxification of the explosive 2,4,6-trinitrotoluene in Arabidopsis: discovery of bifunctional O- and C-glucosyltransferases *Plant J*. 56:963–974.

GAO, M.-J., LYDIATE, D. J., LI, X., LUI, H., GJETVAJ, B., HEGEDUS, D. D., and ROZWADOWSKI, K. 2009. Repression of seed maturation genes by a trihelix transcriptional repressor in *Arabidopsis* seedlings. *Plant Cell* 21:54–71.

HAYASHI, K., KAMIO, S., OONO, Y., TOWNSEND, L. B., and NOZAKI, H. 2009. Toyocamycin specifically inhibits auxin signaling mediated by SCFTIR1 pathway. *Phytochemistry* 70:190–197.

JEFFERSON, R. A. 1987. Assaying chimeric gene in plant: The uidA gene fusion system. *Plant Mol. Biol. Rep*. 5:387–405.

KAI, K., MIZUTANI, M., KAWAMURA, N., YOMAMOTO, R., TAMAI, M., YAMAGUCHI, H., SAKATA, K., and SHIMIZU, B. 2008. Scopoletin is biosynthesized via ortho-hydroxylation of feruloyl CoA by a 2-oxoglutarate-dependent dioxygenase in *Arabidopsis thaliana*. *Plant J*. 55:989–999.

KOSTOVA, I., RALEVA, S., GENOVA, P., and ARGIROVA, R. 2006. Structure-activity relationships of synthetic coumarin as HIV-1 inhibitors. *Bioinorganic Chem. Appl*. p1–9.

LI, X., GAO, P., GRUBER, M. Y., WESTCOTT, N., and GJETVAJ, B. 2009a. Analysis of the metabolome and transcriptome of *Brassica carinata* seedlings after lithium chloride exposure. *Plant Sci*. 177:68–80.

LI, X., LIU, Z., CHEN, Y., WANG, L., ZHENG, Y., SUN, G., and RUAN, C. 2009b. Rubiacordone A: A new anthraquinone glycoside from the roots of Rubia cordifolia. *Molecules* 14:566–572.

LI, X., QIN, J.-C., WANG, Q.-Y., WU, X., PAN, H.-Y., GRUBER, M. Y., and GAO, M.-J. 2011. Metabolic engineering of isoflavone genistein in *Brassica napus* with soybean isoflavone synthase. *Plant Cell Rep*. (Online First doi:10.1007/s00299-011-1052-8).

LIM, E. K., BALDAUL, S., LI, Y., ELISA, L., WORRALL, D., SPENCER, S. P., JACKSON, R. G., TAGUCHI, G., ROSS, J., and BOWLES, D. J. 2003. Evolution of substrate recognition across a multigene family of glycosyltransferases in *Arabidopsis*. *Glycobiology* 13:139–145.

LUPINI, A., SORGONÀ, A., MILLER, A. J., and ABENAVOLI, M. R. 2010. Short-term effects of coumarin along the maize primary root axis. *Plant Signal Behav.* 5(11).

MISHRA, B. S., SINGH, M., AGGRAWAL, P., and LAXMI, A. 2009. Glucose and auxin signaling interaction in controlling *Arabidopsis thaliana* seedlings root growth and development. *PLoS One* 4:e4502.

MOTES, C. M., PECHTER, P., YOO, C. M., WANG, Y., CHAPMAN, K. D., and BLANCAFLOR, E. B. 2005. Differential effects of two phospholipase D inhibitor, 1-butanol and N-acylethanolamine, on *in vivo* cytoskeletal organization and Arabidopsis seedling growth. *Protoplasma* 226:109–123.

NIBAU, C., GIBBS, D. J., and COATES, J. C. 2008. Braching out in new directions: the control of root architecture by lateral root formation. *New Phytol*. 179:595–614.

NICK, P., HAN, M. J., and AN, G. 2009. Auxin stimulates its own transport by shaping actin filaments. *Plant Physiol*. 151:155–167.

OSMONT, K. S., SIBOUT, R., and HARDTKE, C. S. 2007. Hidden braches: developments in root system architecture. *Ann. Rev. Plant Biol*. 58:93–113.

PETRÁSEK, J. and FRIML, J. 2009. Auxin transport routes in plant development. *Development* 136:2675–2688.

PERET, B., DE RYBEL, B., CASIMIRO, I., BENKOVA, E., SWARUP, R., LAPLAZE, L., BEECKMAN, T., and BENNETT, M.J. 2009. *Arabidopsis* lateral root development: an emerging story. *Trends Plant Sci*. 14:399–408.

SVENSSON, S. B. 1971. The effect of coumarin on root growth and root histology. *Physiol*. *Plant*. 24: 446–470.

ULMASOV, T., MURFETT, J., HAGEN, G., and GUILFOYLE, T. J. 1997. Aux/IAA proteins repress expression of reporter genes containing natural and highly active synthetic auxin response elements. *Plant Cell* 9:1963–1971.

VANNESTE, S., and FRIML, J. 2009. Auxin: a trigger for change in plant development. *Cell* 136:1005–1016.

WALSH, D. P., and CHANG, Y. T. 2006. Chemical genetics. *Chem. Review* 106:2476–2530.

ZHAO, J., BUCHWALDT, L., RIMMER, S. R., SHARPE, A., MCGREGOR, L., BEKKAOUI, D., and HEGEDUS, D. 2009. Patterns of differential gene expression in *Brassica napus* cultivars infected with *Sclerotinia sclerotiorum*. *Mol. Plant. Pathol*. 10:635–649.

ZHAO, Y., CHRISTENSEN, S. K., FANKHAUSER, C., CASHMAN, J. R., COHEN, J. D., WEIGEL, D., and CHORY, J. 2001. A role for flavin monooxygenase-like enzymes in auxin biosynthesis. *Science* 291:306–309.